Radiative decays of decuplet hyperons

Georg Wagner,[1,2,*] A. J. Buchmann,[2,†] and Amand Faessler[2,‡]

[1]*Centre for the Subatomic Structure of Matter (CSSM), University of Adelaide, Australia 5005*

[2]*Institut für Theoretische Physik, Universität Tübingen, Auf der Morgenstelle 14, 72076 Tübingen, Germany*

(Received 14 May 1998)

We calculate the radiative decay widths of decuplet hyperons in a chiral constituent quark model including electromagnetic exchange currents between quarks. Exchange currents contribute significantly to the $E2$ transition amplitude, while they largely cancel for the $M1$ transition amplitude. Strangeness suppression of the radiative hyperon decays is found to be weakened by exchange currents. Differences and similarities between our results and other recent model predictions are discussed. [S0556-2813(98)06209-8]

PACS number(s): 12.39.Pn, 13.30.−a, 13.40.Hq, 14.20.Jn

I. INTRODUCTION

Electromagnetic transitions in baryons provide not only information on the importance of exchange currents but also on the effective quark-quark interaction. In the context of potential models, electromagnetic gauge invariance relates the two-body terms of the quark model Hamiltonian (potentials) to the two-body terms in the current operator (exchange currents). The excitation spectrum and electromagnetic transition amplitudes of baryons are thus intimately connected. Recently, several works [1–5] have systematically discussed two-body exchange current effects on electromagnetic observables. A good example for the importance of exchange currents is the $C2$ ($E2$) multipole amplitude in the $\gamma N \leftrightarrow \Delta$ transition. While constituent quark model calculations using D-state admixtures underpredict this observable by a factor of 3 or more, exchange currents give the correct empirical quadrupole transition amplitude [4].

Here, we briefly report on the first study of exchange current effects on the radiative decays of all decuplet hyperons. Theoretical studies of radiative hyperon decays have been performed in the pioneering work of Lipkin [6], the quark model (without exchange currents) [7], $SU_F(3)$ Skyrme model approaches [8–10], chiral bag models [11], heavy baryon chiral perturbation theory [12], or quenched lattice calculations [13]. Current experimental programs aim at a detailed measurement of the radiative decays of some Σ^* and Ξ^* hyperons [14].

Radiative decays of hyperons are interesting for several reasons. In previous quark model calculations of decuplet hyperon decays [7], which neglect exchange currents and D-state admixtures, all decays are pure $M1$ transitions. Here, we find that the inclusion of exchange currents leads in all cases to nonvanishing $E2/M1$ ratios. The comparison of our results with other model predictions and experimental data may not only provide another signal of exchange currents inside baryons but may even help to pin down the relative importance of vector (gluon) vs pseudoscalar degrees of freedom in the effective quark-quark interaction at low energies.

Radiative hyperon decays are sensitive to $SU_F(3)$ flavor symmetry breaking and strangeness suppression. The decay widths of the negatively charged hyperons $\Sigma^{*-} \to \gamma \Sigma^-$ and $\Xi^{*-} \to \gamma \Xi^-$ would be zero, if $SU_F(3)$ flavor symmetry were realized in nature. It has been speculated [8] that these two decays remain almost forbidden even after $SU_F(3)$ symmetry breaking. Strangeness suppression, i.e., the decrease of the decay amplitude with increasing strangeness of the hyperon, is best studied by comparing transitions involving wave functions which are identical except for the replacement of d quarks by s quarks. The decays $\gamma n \leftrightarrow \Delta^0$ and $\gamma \Xi^0 \leftrightarrow \Xi^{*0}$ are particularly suited, because the strangeness content increases by two units.

II. MODEL DESCRIPTION

As a consequence of the spontaneously broken chiral symmetry of low-energy QCD, constituent quarks and the pseudoscalar (PS) mesons emerge as relevant degrees of freedom in hadron physics. The chiral quark model Hamiltonian in the case of three nonequal quark masses m_i is

$$H = \sum_{i=1}^{3} \left(m_i + \frac{\mathbf{p}_i^2}{2m_i} \right) - \frac{\mathbf{P}^2}{2M} - a_c \sum_{i<j}^{3} \boldsymbol{\lambda}_i^C \cdot \boldsymbol{\lambda}_j^C \, (\mathbf{r}_i - \mathbf{r}_j)^2$$
$$+ \sum_{i<j}^{3} V^{\text{res}}(\mathbf{r}_i, \mathbf{r}_j). \tag{1}$$

Here, $\boldsymbol{\lambda}_i^C \cdot \boldsymbol{\lambda}_j^C = \sum_{a=1}^{8} \lambda_i^{C,a} \lambda_j^{C,a}$ is a scalar product in color space, where $\lambda_i^{C,a}$ are the Gell-Mann $SU_C(3)$ color matrices. A quadratic confinement potential is used. The radial form of the confinement potential is, according to our experience, not crucial for the discussion of hadronic ground state properties. We will discuss the dependence of our results on different types of confinement interactions, e.g., linear confinement, elsewhere. Hamiltonian (1) is described for the two-flavor case in Refs. [1,3,4]. The residual interactions V^{res} comprise one-gluon exchange (OGE) in the common Fermi-Breit form without retardation corrections [15],

———————

*Electronic address: georg.wagner@uni-tuebingen.de

†Electronic address: alfons.buchmann@uni-tuebingen.de

‡Electronic address: amand.faessler@uni-tuebingen.de

TABLE I. Individual contributions of Hamiltonian (1) to baryon masses. All quantities are given in MeV. Experimental values average over particles with different charge.

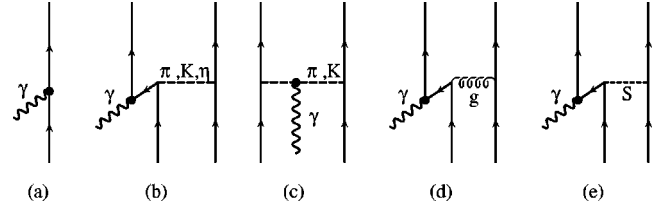|	$\Sigma_i m_i$	E_{kin}	V_{conf}	V_{gluon}	$V_{PS\text{-}octet}$	V_σ	m_B	m_{expt} [16]
p,n	939	497	204	-531	-115	-54	939	939
Σ	1195	497	173	-562	-51	-65	1188	1193
Λ	1195	497	173	-588	-88	-65	1124	1116
Ξ	1451	497	143	-652	-45	-78	1316	1318
Δ	939	497	204	-326	-27	-54	1232	1232
Σ^*	1195	497	173	-423	-18	-65	1359	1385
Ξ^*	1451	497	143	-561	-13	-78	1439	1535
Ω^-	1707	497	112	-595	-12	-95	1615	1672

FIG. 1. (a) Impulse approximation, (b) PS-meson-pair current (π, K, η), (c) PS-meson in-flight current, (d) gluon-pair current, and (e) scalar-exchange current (confinement and σ exchange).

$$V^{OGE} = \frac{\alpha_s}{4} \boldsymbol{\lambda}_i^C \cdot \boldsymbol{\lambda}_j^C \left(\frac{1}{r} - \frac{\pi}{2} \left(\frac{1}{m_i^2} + \frac{1}{m_j^2} + \frac{4}{3} \frac{\boldsymbol{\sigma}_i \cdot \boldsymbol{\sigma}_j}{m_i m_j} \right) \delta(\mathbf{r}) \right.$$
$$- \frac{1}{4 m_i m_j} (3\boldsymbol{\sigma}_i \cdot \hat{\mathbf{r}} \boldsymbol{\sigma}_j \cdot \hat{\mathbf{r}} - \boldsymbol{\sigma}_i \cdot \boldsymbol{\sigma}_j) \frac{1}{r^3}$$
$$- \frac{1}{8 r^3} \left\{ 3 \left[\mathbf{r} \times \left(\frac{\mathbf{p}_i}{m_i} - \frac{\mathbf{p}_j}{m_j} \right) \right] \cdot \left(\frac{\boldsymbol{\sigma}_i}{m_i} + \frac{\boldsymbol{\sigma}_j}{m_j} \right) \right.$$
$$\left. \left. - \left[\mathbf{r} \times \left(\frac{\mathbf{p}_i}{m_i} + \frac{\mathbf{p}_j}{m_j} \right) \right] \cdot \left(\frac{\boldsymbol{\sigma}_i}{m_i} - \frac{\boldsymbol{\sigma}_j}{m_j} \right) \right\} \right), \quad (2)$$

and the generalized chiral interactions due to PS meson exchange.

$$V^{PS} = (\boldsymbol{\sigma}_i \cdot \boldsymbol{\nabla}_\mathbf{r})(\boldsymbol{\sigma}_j \cdot \boldsymbol{\nabla}_\mathbf{r}) \left\{ \sum_{a=1}^{3} \lambda_i^a \cdot \lambda_j^a \widetilde{V}_\pi(r) + \sum_{a=4}^{7} \lambda_i^a \cdot \lambda_j^a \widetilde{V}_K(r) \right.$$
$$\left. + \lambda_i^8 \cdot \lambda_j^8 \widetilde{V}_\eta(r) \right\},$$

$$\widetilde{V}_\gamma = \frac{g_{PSqq}^2}{4\pi} \frac{\Lambda_\gamma^2}{\Lambda_\gamma^2 - m_\gamma^2} \frac{1}{4 m_i m_j} \left(\frac{\exp(-m_\gamma r)}{r} - \frac{\exp(-\Lambda_\gamma r)}{r} \right),$$
$$\gamma = \pi, K, \eta. \quad (3)$$

The λ_i^a are the $SU_F(3)$ flavor matrices. In Eq. (3), experimental pseudoscalar meson masses $m_\pi = 138$ MeV, $m_K = 495$ MeV, $m_\eta = 547$ MeV, and a universal cutoff $\Lambda_\pi = \Lambda_K = \Lambda_\eta = 4.2$ fm^{-1} are used. The quark-meson coupling constant g_{PSqq} is related in the usual way to the pion-nucleon coupling. We furthermore include the σ meson as the chiral partner of the pion [3], whereas we neglect the heavier ($m \simeq 1$ GeV) scalar partners of the kaon and η.

As in Ref. [3], we use spherical $(0s)^3$ oscillator states for the baryon wave functions. For the chosen quark masses $m_u = m_N/3 = 313$ MeV and $m_u/m_s = 0.55$, the effective quark-gluon coupling α_c, the confinement strength a_c, and the wave function oscillator parameter b_N are determined from the empirical baryon masses. Our parameters are very similar to those in Ref. [3], and the octet baryon magnetic moments are, with the exception of the Σ^+ magnetic moment, well described. Results for the individual potential contributions to the baryon masses are given in Table I.

While our results for ground state hyperon properties are satisfying, the strong one-gluon exchange seems to prevent a simultaneous description of the low-lying Roper and the negative parity resonances of the hyperons [17]. The Roper resonances have been attributed to different kinds of quark and/or meson dynamics, and their interpretation as pure three-quark configurations is far from being firmly established. Here, we focus on electromagnetic decay amplitudes of decuplet hyperons in order to obtain further information on the relative importance of pseudoscalar and vector meson exchange between quarks.

The electromagnetic currents corresponding to the Hamiltonian (1) are constructed by a nonrelativistic reduction of the Feynman diagrams [1,4,3] shown in Fig. 1. The spatial exchange currents satisfy the nonrelativistic continuity equation with the exchange potentials in Eq. (1) [1]. Previous quark model calculations of hyperon decays [7] were performed in the impulse approximation, and only the one-body quark current of Fig. 1(a) was considered. The PS-meson pair current $\mathbf{j}_{PSq\bar{q}}$ and in-flight current $\mathbf{j}_{\gamma PS}$ shown in Figs. 1(b) and 1(c) are given by

$$\mathbf{j}_{PSq\bar{q}} = e\{\exp(i\mathbf{q} \cdot \mathbf{r}_i) \boldsymbol{\sigma}_i (\boldsymbol{\sigma}_j \cdot \boldsymbol{\nabla}_\mathbf{r})[(\boldsymbol{\tau}_i \times \boldsymbol{\tau}_j)_z \widetilde{V}_\pi + (\lambda_4^i \lambda_5^j - \lambda_5^i \lambda_4^j) \widetilde{V}_K] + (i \leftrightarrow j)\} + \frac{ie}{4} \left\{ \frac{\exp(i\mathbf{q} \cdot \mathbf{r}_i)}{m_i^2} (\mathbf{q} \times \boldsymbol{\nabla}_\mathbf{r})(\boldsymbol{\sigma}_j \cdot \boldsymbol{\nabla}_\mathbf{r}) \right.$$

$$\times \left[\left(\frac{\boldsymbol{\tau}_i \cdot \boldsymbol{\tau}_j}{3} + \tau_z^{(j)} \right) \widetilde{V}_\pi + \frac{1}{3} (\lambda_4^i \lambda_4^j + \lambda_5^i \lambda_5^j - 2\lambda_6^i \lambda_6^j - 2\lambda_7^i \lambda_7^j) \widetilde{V}_K + \left(-\frac{1}{3} \lambda_8^i \lambda_8^j + \frac{2}{3\sqrt{3}} \lambda_8^j + \frac{1}{\sqrt{3}} \lambda_3^i \lambda_8^j \right) \widetilde{V}_\eta \right] + (i \leftrightarrow j) \bigg\},$$

$$\mathbf{j}_{\gamma PS} = e(\boldsymbol{\sigma}_i \cdot \boldsymbol{\nabla}_\mathbf{r})(\boldsymbol{\sigma}_j \cdot \boldsymbol{\nabla}_\mathbf{r}) \int_{-1/2}^{1/2} d\nu \exp[i\mathbf{q} \cdot (\mathbf{R} - \nu\mathbf{r})][(\boldsymbol{\tau}_i \times \boldsymbol{\tau}_j)_z \vec{\widetilde{V}}_\pi + (\lambda_4^i \lambda_5^j - \lambda_5^i \lambda_4^j) \vec{\widetilde{V}}_K],$$

TABLE II. Transition magnetic moments of decuplet baryons. The impulse (μ_{imp}) and the various exchange current contributions are listed separately: gluon pair ($\mu_{gq\bar{q}}$), PS-meson pair ($\mu_{\text{PS}q\bar{q}}$) and PS meson in flight ($\mu_{\gamma\text{PS}}$), confinement (μ_{conf}) and σ pair (μ_σ). Skyrme model results from [8] and lattice calculation results from [13] (with phase conventions adapted to our calculation) are given in the last two columns for comparison. The latter are rescaled to the proton magnetic moment, which is too small — $\mu_p \simeq 2.3\mu_N$ — on the lattice. Experimentally known is only the nonstrange $\Delta^+ \to \gamma p$ transition magnetic moment. From the empirical helicity amplitudes and Eq. (53) in Ref. [4] one obtains $\mu_{\Delta^+\to p}^{\text{expt}} = 3.58(9)\mu_N$ [16], $\mu_{\Delta^+\to p}^{\text{expt}} = 3.68(9)\mu_N$ [19], and $\mu_{\Delta^+\to p}^{\text{expt}} = 3.47\mu_N$ [21]. All transition magnetic moments are given in units of nuclear magnetons $\mu_N = e/2M_N$.

	μ_{imp}	$\mu_{gq\bar{q}}$	$\mu_{\text{PS}q\bar{q}}$	$\mu_{\gamma\text{PS}}$	μ_{conf}	μ_σ	μ_{tot}	$|\mu_{\text{Skyrme}}|$ [8]	μ_{lattice} [13]
$\gamma N \leftrightarrow \Delta$	2.828	0.292	−0.274	0.586	−1.228	0.327	2.533	2.388	2.83 ± 0.49
$\gamma\Sigma^+ \leftrightarrow \Sigma^{*+}$	2.404	0.366	−0.068	0.097	−0.822	0.291	2.267	1.510	2.22 ± 0.30
$\gamma\Sigma^0 \leftrightarrow \Sigma^{*0}$	−0.990	−0.095	0.036	−0.049	0.278	−0.105	−0.924	0.612	-0.91 ± 0.11
$\gamma\Sigma^- \leftrightarrow \Sigma^{*-}$	−0.424	−0.176	−0.004	0	0.267	−0.082	−0.419	0.286	-0.39 ± 0.08
$\gamma\Lambda \leftrightarrow \Sigma^{*0}$	2.449	0.371	−0.212	0.366	−0.944	0.323	2.354	1.814	—
$\gamma\Xi^0 \leftrightarrow \Xi^{*0}$	2.404	0.431	−0.117	0.097	−0.716	0.329	2.428	1.469	2.12 ± 0.24
$\gamma\Xi^- \leftrightarrow \Xi^{*-}$	−0.424	−0.190	0.009	0	0.235	−0.090	−0.460	0.211	-0.36 ± 0.06

$$\vec{V}_\gamma = \frac{g_{\text{PS}qq}^2}{4\pi} \frac{\Lambda_\gamma^2}{\Lambda_\gamma^2 - m_\gamma^2} \frac{1}{4m_i m_j} \left(\vec{z}_{m_\gamma} \frac{\exp(-L_{m_\gamma} r)}{L_{m_\gamma} r} - \vec{z}_{\Lambda_\gamma} \frac{\exp(-L_{\Lambda_\gamma} r)}{L_{\Lambda_\gamma} r} \right), \quad \gamma = \pi, K,$$

$$\vec{z}_m = L_m \vec{r} + i\nu r \vec{q}, \quad L_m(q,\nu,m) = \sqrt{\frac{q^2}{4}(1 - 4\nu^2) + m^2}. \tag{4}$$

In Eqs. (4) $\mathbf{r}_i$, $\boldsymbol{\sigma}_i$, and $\boldsymbol{\tau}_i$ are coordinate, spin, and isospin of the ith quark, $\mathbf{r} = \mathbf{r}_i - \mathbf{r}_j$, and $\mathbf{q}$ is the photon momentum. The remaining currents can be found in [3].

Siegert's theorem connects the $C2$ and $E2$ transition amplitudes in the long-wavelength limit and allows one to calculate the $E2$ transition form factor at small momentum transfers from the charge density $\rho(\mathbf{q})$. For spherical wave functions, only the gluon- and PS-meson-pair charge density operators contribute:

$$\rho_{\text{PS}q\bar{q}} = \frac{ie}{2} \left\{ \frac{\exp(i\mathbf{q}\cdot\mathbf{r}_i)}{m_i} (\boldsymbol{\sigma}_i \cdot \mathbf{q})(\boldsymbol{\sigma}_j \cdot \nabla_\mathbf{r}) \left[\left(\frac{\boldsymbol{\tau}_i \cdot \boldsymbol{\tau}_j}{3} + \tau_z^{(j)} \right) \widetilde{V}_\pi + \frac{1}{3}(\lambda_4^i \lambda_4^j + \lambda_5^i \lambda_5^j - 2\lambda_6^i \lambda_6^j - 2\lambda_7^i \lambda_7^j)\widetilde{V}_K \right. \right.$$

$$\left. \left. + \left(-\frac{1}{3}\lambda_8^i \lambda_8^j + \frac{2}{3\sqrt{3}}\lambda_8^j + \frac{1}{\sqrt{3}}\lambda_3^i \lambda_8^j \right)\widetilde{V}_\eta \right] + (i \leftrightarrow j) \right\},$$

$$\rho_{gq\bar{q}} = -i\frac{\alpha_s}{16} \boldsymbol{\lambda}_i^C \cdot \boldsymbol{\lambda}_j^C \left\{ \frac{e_i}{m_i} e^{i\mathbf{q}\cdot\mathbf{r}_i} \left[\frac{\mathbf{q}\cdot\mathbf{r}}{m_i^2} + \left(\frac{\boldsymbol{\sigma}_i}{m_i} \times \mathbf{q} \right) \cdot \left(\frac{\boldsymbol{\sigma}_j}{m_j} \times \mathbf{r} \right) \right] + (i \leftrightarrow j) \right\} \frac{1}{r^3}. \tag{5}$$

Their tensorial spin structure in Eqs. (5) allows for a double spin flip of the two participating quarks $\sigma_i^+ \sigma_j^-$ as the only mechanism by which a $C2$ (or $E2$) photon can be absorbed [4].

Our $M1$ and $C2$ transition form factors are defined as

$$F_{M1}(\mathbf{q}^2) = \frac{4\sqrt{3\pi}M_N}{q} \left\langle J^P = \frac{3^+}{2}, M_J = \frac{1}{2} \left| \frac{1}{4\pi}\int d\Omega_\mathbf{q} \cdot Y_{1\text{-}1}(\hat{\mathbf{q}})\mathbf{j}^+(\mathbf{q}) \right| J^P = \frac{1^+}{2}, M_J = \frac{1}{2} \right\rangle,$$

$$F_{C2}(\mathbf{q}^2) = -\frac{12\sqrt{5\pi}}{q^2} \left\langle J^P = \frac{3^+}{2}, M_J = \frac{1}{2} \left| \frac{1}{4\pi}\int d\Omega_\mathbf{q} \cdot Y_{20}(\hat{\mathbf{q}})\rho(\mathbf{q}) \right| J^P = \frac{1^+}{2}, M_J = \frac{1}{2} \right\rangle. \tag{6}$$

III. RESULTS AND DISCUSSION

The one- and two-body current contributions to the $M1$ transition moments $\mu = F_{M1}(q^2=0)$ are given in Table II. Individual exchange current contributions are as large as 60% of the impulse approximation result.

As for the octet baryon magnetic moments [3], we ob-serve substantial cancellations between the gluon-pair and the scalar-pair currents (confinement and one-sigma ex-change) for all decays. Because of partial cancellations be-tween the PS meson in flight and the PS-meson-pair term, the total PS-meson contribution to the $M1$ amplitude is small. Nevertheless, the PS-meson contribution is important. It reduces the strong quark-gluon coupling constant and thus

TABLE III. Transition quadrupole moments of decuplet baryons. The gluon-pair ($Q_{gq\bar{q}}$) and individual PS-meson (π, K, η) exchange current contributions are listed separately. Skyrme model results from [8] and lattice calculation results from [13] (with phase conventions adapted to our calculation) are given in the last two columns for comparison. The experimental transition quadrupole moments as extracted from the empirical helicity amplitudes according to Eq. (53) in Ref. [4]: $Q_{N\to\Delta}^{\text{expt}} = -0.043(40)$ fm^2 [16], $Q_{N\to\Delta}^{\text{expt}} = -0.105(16)$ fm^2 [19], and $Q_{N\to\Delta}^{\text{expt}} = -0.085(13)$ fm^2 [20,21]. All transition quadrupole moments are given in fm^2.

	$Q_{gq\bar{q}}$	$Q_{\pi q\bar{q}}$	$Q_{Kq\bar{q}}$	$Q_{\eta q\bar{q}}$	Q_{tot}	$|Q_{\text{Skyrme}}|$ [8]	Q_{lattice} [13]
$\gamma N \leftrightarrow \Delta$	-0.058	-0.027	0	-0.004	-0.089	0.051	-0.073 ± 0.190
$\gamma \Sigma^+ \leftrightarrow \Sigma^{*+}$	-0.051	-0.036	0.005	-0.009	-0.091	0.025	-0.141 ± 0.176
$\gamma \Sigma^0 \leftrightarrow \Sigma^{*0}$	0.016	0.009	0.002	0.002	0.030	0.009	0.041 ± 0.068
$\gamma \Sigma^- \leftrightarrow \Sigma^{*-}$	0.018	0.018	-0.010	0.006	0.032	0.008	0.050 ± 0.025
$\gamma \Lambda \leftrightarrow \Sigma^{*0}$	-0.041	0	-0.013	0.006	-0.047	0.035	—
$\gamma \Xi^0 \leftrightarrow \Xi^{*0}$	-0.035	0	-0.005	0.001	-0.039	0.023	-0.059 ± 0.074
$\gamma \Xi^- \leftrightarrow \Xi^{*-}$	0.012	0	0.010	-0.006	0.016	0.005	0.033 ± 0.014

the gluon-exchange current contribution.

In the impulse approximation, $\text{SU}_F(3)$ symmetry breaking, i.e., the fact that $m_u/m_s = 0.55-0.6$ as suggested by the octet magnetic moments [3], leads to a reduction of the transition magnetic moments with increasing strangeness content of the hyperon. We find that this strangeness suppression is for all six strange decays considerably reduced when exchange currents are included. In particular, the reduction of the $\gamma\Xi^0\leftrightarrow\Xi^{*0}$ $M1$ transition moment $\mu_{\text{imp}}^{\gamma\Xi^0\leftrightarrow\Xi^{*0}} = 2.404\mu_N$ with respect to the $\gamma n\leftrightarrow\Delta^0$ transition magnetic moment $\mu_{\text{imp}}^{\gamma n\leftrightarrow\Delta^0} = 2.828\mu_N$, which is observed in the impulse approximation, practically disappears when exchange currents are included, and we obtain $\mu_{\text{tot}}^{\gamma n\leftrightarrow\Delta^0} \simeq \mu_{\text{tot}}^{\gamma\Xi^0\leftrightarrow\Xi^{*0}} = 2.428\mu_N$. Strangeness suppression is strong in the Skyrme model calculation of [8], while the lattice results from [13] agree reasonably well with our predictions.

An interesting comparison can be made for the $M1$ moments of the $\gamma\Sigma^+\leftrightarrow\Sigma^{*+}$ and $\gamma\Xi^0\leftrightarrow\Xi^{*0}$ transitions, as well as for the $\gamma\Sigma^-\leftrightarrow\Sigma^{*-}$ and $\gamma\Xi^-\leftrightarrow\Xi^{*-}$ transitions. They are pairwise equal in the impulse approximation (see the first column in Table II), and would also be equal after inclusion of exchange currents if $\text{SU}_F(3)$ flavor symmetry was exact. Gluon- and scalar-exchange currents lead to deviations from this equality of about 10%. Less pronounced deviations from $\text{SU}_F(3)$ (in the opposite direction) are seen in the lattice results, whereas the Skyrme model shows a near equality for the $M1$ moments of the $\gamma\Sigma^+\leftrightarrow\Sigma^{*+}$ and $\gamma\Xi^0\leftrightarrow\Xi^{*0}$ transitions, but a large difference for $\gamma\Sigma^-\leftrightarrow\Sigma^{*-}$ and $\gamma\Xi^-\leftrightarrow\Xi^{*-}$ $M1$ transitions.

In addition, we point out that the transition magnetic moments for the negatively charged hyperons ($\sim -0.4\mu_N$) deviate considerably from the $\text{SU}_F(3)$ flavor-symmetric value 0, when the quark mass ratio $m_u/m_s = 0.55$ is used. If $\text{SU}_F(3)$ symmetry were exact, these amplitudes would vanish even when exchange currents are included. In contrast to the Skyrme model [8], we find a stronger $\text{SU}_F(3)$ symmetry violation for these decays.

We observe that the hyperon transition quadrupole moments shown in Table III receive large contributions from the PS-meson- and gluon-pair diagrams of Figs. 1(b) 1(d). We recall that the $E2$ transition moments resulting from the one-body charge and the spin-independent scalar exchange

charge operators are exactly zero for spherical valence quark wave functions. The transition $E2$ moments for the negatively charged hyperons Ξ^{*-} and Σ^{*-} deviate from the $\text{SU}_F(3)$ flavor-symmetric value 0. Our results are in absolute magnitude mostly larger than the Skyrme model results [8,9], but somewhat smaller than the lattice results [13].

The helicity amplitudes $A_{3/2}(\mathbf{q}^2)$ and $A_{1/2}(\mathbf{q}^2)$ of the radiative hyperon decays can be expressed as linear combinations of the $M1$ and $E2$ transition form factors (6) [18]. The $E2/M1$ ratio of the transition amplitudes is defined as

$$\frac{E2}{M1} \equiv \frac{1}{3}\frac{A_{1/2}(E2)}{A_{1/2}(M1)} \equiv -\frac{A_{3/2}(E2)}{A_{3/2}(M1)} = \frac{\omega M_N}{6}\frac{F_{C2}(\mathbf{q}^2=0)}{F_{M1}(\mathbf{q}^2=0)}. \quad (7)$$

The last equality is a consequence of Siegert's theorem and has been derived in Ref. [4]. The resonance frequency ω is given in the c.m. system of the decaying hyperon by $\omega = (M_{\text{decuplet}}^2 - M_{\text{octet}}^2)/(2M_{\text{decuplet}})$. Following Giannini [18], partial decay widths are calculated:

$$\Gamma_{E2,M1} = \frac{\omega^2}{\pi}\frac{M_{\text{octet}}}{M_{\text{decuplet}}}\frac{2}{2J+1}\{|A_{3/2}(E2,M1)|^2$$
$$+ |A_{1/2}(E2,M1)|^2\},$$
$$J = 3/2, \quad (8)$$

with, again, $|E2/M1| = \sqrt{\Gamma_{E2}/3\Gamma_{M1}}$.

In Table IV, helicity amplitudes $A_{3/2}(\mathbf{q}^2=0)$ and $A_{1/2}(\mathbf{q}^2=0)$, $E2/M1$ ratios, Eq. (7), and the radiative decay widths $\Gamma = \Gamma_{E2} + \Gamma_{M1}$, Eq. (8), are compared with previous quark model calculations performed in the impulse approximation [7], the $\text{SU}_F(3)$ Skyrme model in the slow rotor approach [8], and the quenched lattice calculation of [13]. Because of cancellations of different exchange current contributions to the $M1$ transition amplitude and the relative smallness of the $E2$ amplitude, the decay width Γ is dominated by the $M1$ impulse approximation. This explains the agreement of the present calculation with the results of [7]. The strong suppression of the total decay width Γ with increasing strangeness seen in the Skyrme model is not repro-

TABLE IV. Helicity amplitudes $A_{3/2}, A_{1/2}$ (in 10^{-3} GeV$^{-1/2}$), radiative decay widths Γ (in keV), and $E2/M1$ ratios (in %) calculated in the present model in comparison with impulse approximation quark model results from [7], $SU_F(3)$ Skyrme model results (slow rotor approach for the kaon fields) from [8], and lattice QCD results from [13]. Note that our results are given at $\mathbf{q}^2 = 0$. Experimentally known are the nonstrange $\gamma N \leftrightarrow \Delta$ helicity amplitudes $A_{3/2}^{\text{expt}} = -(257 \pm 8) \times 10^{-3}$ GeV$^{-1/2}$ and $A_{1/2}^{\text{expt}} = -(141 \pm 5) \times 10^{-3}$ GeV$^{-1/2}$, and the decay width $\Gamma_{\Delta \to \gamma N}^{\text{expt}} = 610 - 730$ keV [16]. The empirical $E2/M1$ ratios for the $\gamma N \leftrightarrow \Delta$ transition are $E2/M1 = -1.5(4)\%$ [16], and $E2/M1 = -2.5(4)\%$ [20], $E2/M1 = -3.0(5)\%$ [19]. If we use the empirical $M1$ amplitude and the calculated $E2$ amplitude, we obtain $E2/M1 = -2.6\%$ (see text).

	Chiral quark model				Quark model [7]		Skyrme [8]		Lattice [13]	
	$A_{3/2}$	$A_{1/2}$	Γ	$E2/M1$	Γ	$E2/M1$	Γ	$E2/M1$	Γ	$E2/M1$
$\gamma N \leftrightarrow \Delta$	-186	-92	350	-3.65	—	—	309	-2.2	430 ± 150	3 ± 8
$\gamma \Sigma^+ \leftrightarrow \Sigma^{*+}$	-138	-71	105	-2.9	104	0	47	-1.2	100 ± 26	5 ± 6
$\gamma \Sigma^0 \leftrightarrow \Sigma^{*0}$	56	29	17.4	-2.3	19	0	7.7	-1.0	17 ± 4	4 ± 6
$\gamma \Sigma^- \leftrightarrow \Sigma^{*-}$	26.1	11.9	3.61	-5.5	2.5	0	1.7	-2.0	3.3 ± 1.2	8 ± 4
$\gamma \Lambda \leftrightarrow \Sigma^{*0}$	-165	-88	265	-2.0	232	0	158	-1.9	—	—
$\gamma \Xi^0 \leftrightarrow \Xi^{*0}$	-154	-84	172	-1.3	—	—	63	-1.3	129 ± 29	2.4 ± 2.7
$\gamma \Xi^- \leftrightarrow \Xi^{*-}$	30	15	6.18	-2.8	—	—	1.3	-2.1	3.8 ± 1.2	7.4 ± 3.0

duced by our calculation. The decay widths calculated in the chiral quark model are closer to the lattice results.

The $E2/M1$ ratios are sensitive to exchange current contributions. Without exchange currents and D-state admixtures they would all be identical to zero. Except for the small $\gamma \Sigma^+ \leftrightarrow \Sigma^{*+}$ $E2/M1$ ratio obtained in [8], the chiral quark model, the lattice calculation, and the Skyrme model produce roughly the same ordering of $E2/M1$ ratios. For five decays, the chiral quark model $E2/M1$ ratios lie between the large lattice and the small Skyrme model results. All models yield large (the largest) $E2/M1$ ratios for the negatively charged states. However, there are important differences. The $\gamma \Sigma^0 \leftrightarrow \Sigma^{*0}$ $E2/M1$ ratio in the Skyrme model approaches is zero [9,10], or almost zero [8], while the $SU_F(3)$ symmetry breaking and the gluon-pair current in our model yield a sizable $E2/M1$ ratio of -2.3%. Similarly, the $E2/M1$ ratio for the $\Sigma^{*-} \to \gamma \Sigma^-$ decay, which is largely due to the gluon-pair exchange current, is with -5.5% almost 3 times larger than the Skyrme model result. The decays of negatively charged hyperons are particularly model dependent [10] due to the smallness of both the $E2$ and $M1$ contributions. In our calculation the gluon contributes strongly to most $E2/M1$ ratios. Their measurements will give information on the importance of *effective* gluon (vector exchange) degrees of freedom in hadrons.

So far experimental data exist only for the nonstrange $\mu_{\Delta^+ \to p}$ decay. We briefly summarize the experimental situation. Most approaches (cf. Tables II and IV) underestimate the empirical transition magnetic moment, $\mu_{\Delta^+ \to p}^{\text{expt}} \simeq 3.58(9) \mu_N$, the helicity amplitudes $A_{3/2}^{\Delta^+ \to p} = -(257 \pm 8) \times 10^{-3}$ GeV$^{-1/2}$, $A_{1/2}^{\Delta^+ \to p} = -(141 \pm 5) \times 10^{-3}$ GeV$^{-1/2}$, and decay width $\Gamma_{\Delta \to \gamma N}^{\text{expt}} = 610 - 730$ keV [16]. Note that these observables are interrelated, and that helicity amplitudes or decay widths are dominated by the transition magnetic moment. According to Eq.(53) of Ref. [4] one obtains, from the empirical helicity amplitudes [16] for the magnetic dipole and charge quadrupole transition form factors at $|\mathbf{q}| = 0$, $F_{M1}(0) = 3.58(9) \mu_N$ and $F_Q(0) = -0.043(40)$ fm^2, respectively, and $E2/M1 = -1.5(4)\%$. Similarly, with the experimental helicity amplitudes of Ref. [19] we obtain $F_{M1}(0) = 3.68(9) \mu_N$, $F_Q(0) = -0.105(16)$ fm^2, and

$E2/M1 = -3.0(5)\%$, while a dispersion theoretical analysis of the Mainz data [20] yields $F_{M1}(0) = 3.47 \mu_N$, $F_Q(0) = -0.085(13)$ fm^2, and $E2/M1 = -2.5(4)\%$. Our calculated values are $F_{M1}(0) = 2.533 \mu_N$, $F_Q(0) = -0.089$ fm^2, and $E2/M1 = -3.65\%$. Our parameter-independent relation [4] between the transition quadrupole moment and the neutron charge radius, $F_Q(0) = r_n^2/\sqrt{2}$, yields $F_Q(0) = -0.083$ fm^2, and the corresponding $E2$ amplitude is in very good agreement with recent measurements. However, the underestimation of the magnetic transition moment persists even after the inclusion of exchange currents. If we replace the calculated transition magnetic moment by the empirical transition magnetic moment of Ref. [16], we obtain $E2/M1 = -2.6\%$, in good agreement with recent experiments. However, this should be taken with some caution because experimentally one measures the *total* $E2$ and $M1$ amplitudes, which include the nonresonant Born terms, whereas we calculate only the *resonant* $N \to \Delta$ $E2$ and $M1$ amplitudes.

IV. SUMMARY

We have studied the radiative decays of decuplet hyperons within a chiral quark model including two-body exchange currents. The present calculation complements and improves the quark model calculations of Ref. [7]. Exchange current effects have been evaluated for the first time for all radiative hyperon decays. Exchange currents have a different influence on the radiative hyperon decay widths and on the $E2/M1$ ratios in these decays. The decay width, governed by the $M1$ transition, is determined by the impulse approximation because of substantial cancellations among the various two-body currents. Exchange currents modify the transition magnetic moments typically by 10% or less. This is consistent with our results for octet baryon magnetic moments [3], where similar cancellation mechanisms have been observed. In contrast, exchange currents are extremely important for the $E2/M1$ ratios. The gluon- and PS-meson-pair charge densities lead via Siegert's theorem to nonzero $E2$ amplitudes for all hyperon decays. The $E2/M1$ ratio for the $\Lambda \to \gamma \Sigma^{*0}$ of -2% comes almost exclusively from the gluon-exchange charge density. Experimental results on the $E2/M1$

ratios for the hyperon decays provide an important test for the relative importance of effective gluon versus pseudo-scalar degrees of freedom in low-energy QCD.

We have indicated that detailed measurements of individual $M1$ and $E2$ transition amplitudes may improve our understanding of $SU_F(3)$ flavor symmetry breaking and help to discriminate between models. We find that the strangeness suppression of the hyperon decay amplitudes is weaker than suggested by a recent Skyrme model calculation [8]. The deviation of the decay widths of the negatively charged hyperons $\Sigma^{*-} \to \gamma \Sigma^-$ and $\Xi^{*-} \to \gamma \Xi^-$ from the $SU_F(3)$-flavor-symmetric value is stronger than in the Skyrme model. Exchange currents weaken the strangeness suppression observed for the transition magnetic moments calculated in the impulse approximation.

ACKNOWLEDGMENTS

[1] A. Buchmann, E. Hernández, and K. Yazaki, Phys. Lett. B **269**, 35 (1991); Nucl. Phys. **A569**, 661 (1994); A. J. Buchmann, Z. Naturforsch. Teil A **52**, 877 (1997).

[2] D. Robson, Nucl. Phys. **A560**, 389 (1993); E. Perazzi, M. Radici, and S. Boffi, *ibid.* **A614**, 346 (1997).

[3] G. Wagner, A. J. Buchmann, and A. Faessler Phys. Lett. B **359**, 288 (1995).

[4] A. J. Buchmann, E. Hernández, and A. Faessler, Phys. Rev. C **55**, 448 (1997); A. J. Buchmann, E. Hernández, U. Meyer, and A. Faessler, *ibid.* (to be published).

[5] U. Meyer, A. J. Buchmann, and A. Faessler, Phys. Lett. B **408**, 19 (1997).

[6] H. J. Lipkin, Phys. Rev. D **7**, 846 (1973).

[7] J. W. Darewych, M. Horbatsch, and R. Koniuk, Phys. Rev. D **28**, 1125 (1983); E. Kaxiras, E. J. Moniz, and M. Soyeur, *ibid.* **32**, 695 (1985); R. K. Sahoo, A. R. Panda, and A. Nath, *ibid.* **52**, 4099 (1995).

[8] T. Haberichter, H. Reinhardt, N. N. Scoccola, and H. Weigel, Nucl. Phys. **A615**, 291 (1997); A. Abada, H. Weigel, and H. Reinhardt, Phys. Lett. B **366**, 26 (1996).

[9] Y. Oh, Mod. Phys. Lett. A **10**, 1027 (1995).

[10] C. L. Schat, C. Gobbi, and N. N. Scoccola, Phys. Lett. B **356**, 1 (1995).

[11] S. Kumano, Phys. Lett. B **214**, 132 (1988); K. Bermuth, D. Drechsel, L. Tiator, and J. B. Seaborn, Phys. Rev. D **37**, 89 (1988); I. Guiasu and R. Koniuk, *ibid.* **36**, 2757 (1987); M. Weyrauch, *ibid.* **35**, 1574 (1987); D. H. Lu, A. W. Thomas, and A. G. Williams, Phys. Rev. C **55**, 3108 (1997).

[12] M. N. Butler, M. J. Savage, and R. P. Springer, Phys. Lett. B **304**, 353 (1993).

[13] D. B. Leinweber, T. Draper, and R. M. Woloshyn, Phys. Rev. D **48**, 2230 (1993).

[14] J. S. Russ, Nucl. Phys. **A585**, 39c (1995); R. A. Schumacher, *ibid.* **A585**, 63c (1995).

[15] A. DeRujula, H. Georgi, and S.L. Glashow, Phys. Rev. D **12**, 147 (1975); R. Koniuk and N. Isgur, *ibid.* **21**, 1868 (1980); N. Isgur and G. Karl, *ibid.* **18**, 4187 (1978); **19**, 2653 (1979).

[16] Particle Data Group, R. M. Barnett *et al.*, Phys. Rev. D **54**, 1 (1996).

[17] L. Ya. Glozman, Z. Papp, and W. Plessas, Phys. Lett. B **381**, 311 (1996).

[18] M. M. Giannini, Rep. Prog. Phys. **54**, 453 (1990).

[19] G. Blanpied *et al.*, Phys. Rev. Lett. **79**, 4337 (1997).

[20] R. Beck *et al.*, Phys. Rev. Lett. **78**, 606 (1997).

[21] O. Hanstein, D. Drechsel, and L. Tiator, Phys. Lett. B **385**, 45 (1996); Nucl. Phys **A632,** 561 (1998).